SCIREA Journal of Chemistry

https://www.scirea.org/journal/Chemistry

August 5, 2019

Volume 4, Issue 3, June 2019

Preparation of magnetic nano carrier for in-vitro delivery of methimazole drug complexed with polyethylene glycol in simulated gastric and simulated body fluids, optimizing by RSM

F. Torki[1,*]

Department of Chemistry, Islamic Azad University, Shahreza Branch, Shahreza, Iran

*Corresponding author email: f.torki58@yahoo.com

Abstract

In this research, a magnetized core-shell was prepared by polymerization of pyrrole in the presence of Fe_3O_4 nanoparticles and was used as a drug carrier for methimazole. The drug was introduced to the carrier as methimazole-polyethylene glycol complex. The parameters affecting the synthesis of the carrier and the effect of pH on the release of the drug were optimized by response surface methodology. The drug and polyethylene glycol amounts were taken as numerical factors in five levels and the pH of the fluid as categorical factor in 2 levels (pH=1.2 for simulated gastric fluid and pH=7.4 for simulated body fluid) was considered. It was concluded that in SGF, slower releasing rate was obtained, and the release of the drug was controlled by PEG while the controlling effect of PEG in SBF was insignificant. The ANOVA results indicated the fitness of the model according to R^2=0.9968.

The model was statistically significant according to the F-value and p-value of 1585.72 and 0.0001 respectively. The F-value of Lack of Fit was not significant (0.68) and implied the fittness of the model. The signal to noise ratio of 51.67 indicated an adequate precision.

Keywords: Magnetized nanocarrier; Drug delivery; Polypyrrole; Polyethylene glycol; Biocompatible; Methimazole

Introduction

Methimazole (MET) is an antithyroid medicine used for long term thyroidism therapy.[1] The medicine has an inhibiting effect on hormone secretion, and reduced the thyroid hormone concentration when enters into the human body. The drug has several side effects including vomiting, diarrhea and lethargy. Some other problems such as leucopoenia, thrombocytopenia hemorrhages and cutaneous facial reactions are associated with overdosing of methimazole.[2]

Delayed and controlled release of drugs can reduce drug side effects, decrease dosage of the drug, and improve patient compliance. These advantages are more useful when the drugs are used for long term treatments (such as methimazole) or for oral medicines that are break down in the gastrointestinal tract. Drug release from drug carrier can be done by different processes including; leaching, diffusion, erosion, and dissolution or combined mechanisms.[3,4] Kinetically, the process of drug delivery, and drug dissolution from a matrix can be interpreted by some kinetic models such as zero-order, first order kinetics, Ritger-Peppas, Avarim or other models.[5]

To control, and manage the drug release, it is necessary to prepare new carriers with developed performance and to optimize the conditions of releasing media.[6]

Polimeric systems such as polyvinyl alcohol and starch[7], hydrogels[8], Poly (lactic-co-glycolic acid (PLGA) nanoparticles[9], and polyketals[10] have been well studied as drug carriers. Zheng et al. [11] used polyethylene glycol (PEG)-polylactic acid polymer as a drug carrier system for

delivery of Honokiol to improve the drug delivery rate and to enhance the therapeutic value of drug which was limited because of poor water solubility. [11]

Regi et al. [12] used different pore sizes of amino functionalized MCM-41 mesoporous silicas as drug carriers for delivery of ibuprofen. They reported that the modification of MCM-41 with amino groups had decreasing effect on the drug delivery rate and the pore size of the modified MCM-41 has no influence on the release of the drug. [12]

SBA-15 mesoporous silica has been studied for Gentamycin drug delivery system by Doadrio et al. [13] and Regi et al. [14]. The powder and disk forms of SBA-15 mesoporous material were payload with the drug. The cumulative release rates from the disk and powder was similar, and the drug release of more than 70% was obtained by both forms of mesoporous within 3 h[13,14].

Application of complexing agent for introducing of the drugs into the carrier can decrease the side effects of the drug and can control the release of the drug [15].

Among the biocompatible polymers, PEG is a water soluble, and non-biodegradable and can be used as a non-ionic polymer in the drug delivery process[16]. Due to its high solubility in polar and non-polar solvents, it has been widely employed as a carrier for hydrophobic and hydrophilic drug molecules and showed a significant effect on the performance of the drug delivery system[17-21]. The conjugation of PEG to thiol, hydroxyl or amide groups of drug molecules has also been reported [16].

The aim of this study is to synthesis a nano carrier with improved performance for controlled and delayed release of methimazole. The drug was loaded on the carrier as methimazole-polyethylene glycol complex. To manage the release performance of the carrier, the influencing variables including; amounts of methimazole and PEG were optimized. The releasing of the drug was studied in simulated gastric fluids (SGF, pH=1.2) and simulated body fluids (SBF, pH=7.4)[22]. The central composite design (CCD) by response surface methodology (RSM) was used to optimize the releasing performance of the synthesized carrier.

2. Experimental

2.1. Materials and methods

The chemicals including ammonium persulphate (APS), pyrrole (PY, C_4H_5N), NaOH, HCl, iron (III) chloride ($FeCl_3.6H_2O$), iron (II) chloride ($FeCl_2.4H_2O$), NaCl, $NaHCO_3$, KH_2PO_4, K_2HPO_4, $C_{2n}H_{4n+2}O_{n+1}$ (PEG_{8000}) and H_2O_2,were prepared from Merck Company (Germany). Methimazole ($C_4H_6N_2S$) was purchased from Hormone Pharmaceutical Company (Iran) as 5 mg pharmaceutical tablet. Characterization of nano carrier was performed by Fourier transformation infrared spectroscopy (FTIR). The spectra were prepared on Nicolet single beam Impact 400D, Japan, in the region of 4000–400 cm^{-1} by use of KBr pellet.

The thermal curve (DSC) of the samples were prepared by a differential scanning calorimeter by use of a Perkin-Elmer thermal analyzer (model SSC-5200, USA) from 25 to 300˚C with heating rate of 10˚Cmin^{-1}. The concentration of MET was determined by fluorescence spectroscopy by use of a Perkin-Elmer instrument, model LS-45, USA. Laboratory shaker incubator (KMC65, Fan Azma, Iran).

2.2. Preparation of nano carrier

Fe_3O_4 nanoparticles were prepared according to the method described by Wang et al [23]. In a three-necked Erlenmeyer flask containing 50.00 mL hydrochloric acid (0.50 M) and equipped with a condenser and nitrogen inlet flow, 0.04 mole of $FeCl_3.6H_2O$ and 0.02 mole of $FeCl_2.4H_2O$ were added. The mixture was stirred at 80˚C and its pH was adjusted to 11.00 by dropwise addition of NaOH. The solution was cooled to ambient temperature; the solid was separated by use of a magnet and thoroughly washed with deionized water. The solid product was dried at 60 ˚C for 8 h [23].

The MET-PEG complex was prepared by inclusion of the drug into PEG by co-precipitation method. Known amount of PEG (0.00 to 0.04 g) and MET (0.01 to 0.04 g) were dissolved in 10 mL of deionized water and the solution was stirred at 45˚C for 2 h until the complex was formed. The mixture was heated on a water bath at 80˚C to dryness [24]. In the same manner, several complexes with different MET/PEG ratio were prepared.

To prepare the magnetized carrier, the synthesized MET-PEG complex was added to 0.1 g of Fe_3O_4, and after adding 0.05 g of APS and 3.0 mL deionized water, the mixture was homogenized under N_2 atmosphere and 0.05 mL of PY was drop wise added to the solution[25]. The mixture was continuously shaken for 8h until the polymerization process was completed. The magnetized nano carriers was separated from solution by use of external magnetic field and dried in vacuum oven at ambient temperature.

2.3. Drug release evaluation; studied by RSM

By RSM design, the optimized values of independent variables including; the amount of PEG and MET, and the pH of the releasing media were obtained by use of CCD which determined the influence and interaction between different variables. By employing of RSM, the optimized process settings to achieve desirable performance of the variables was obtained, and the consumption of chemicals, the number of experiments and the time was saved. The coefficients of a quadratic model by adjusting 5 levels for each factors; -α, -1, 0, 1, and +α was estimated by CCD. Two numerical independent factor; (amount of PEG and MET in 5

levels) and 1 categorical independent factor (pHs of release media in 2 levels; (pH 1.2) for simulated gastric fluids (SGF) and (pH 7.4) for simulated body fluids (SBF)) and two blocks were designed by Expert Design software.

To evaluate the response variable (depended factor), the magnetized nano carrier was put in contact with 30 mL of simulated media. The samples were shaken in a laboratory incubator at 37 ˚C. The sampling was done though pre-determined time schedule and equivalent volume of fresh solution was replace after each sampling step. The fluorescence intensity of each sample which was directly proportional to the released amount of MET into the media was determined by fluorescence spectroscopy method. The instrument was put on full scan mode, and the excitation of the sample was performed at 400 nm. The emission peaks were observed at λ_{em} 600-900 nm with the maximum intensity at 806 nm. The measurement was continued until the fluorescence intensity became constant. The correction factor for dilution of the samples was calculated by the following equation. [26]

$$R_n = R_n^0 + \sum_{i=1}^{n=1} R_i^0 \times \frac{V_s}{V_i} \quad (1)$$

Where, R_n^0 and R_i^0 are response in zero and t time and *Vs* and *Vi* are sampling volume and total volume of solution respectively.

The calibration curve was constructed by use of standard MET solutions in the concentration range of 5.0-1000 g.L^{-1}. The R^2 value of calibration curve was 0.992 and linear range of two order of magnitude was obtained. The fluorescence intensity of each sample was used as the response for each run of CCD design. The percentage of drug release was calculated by Eq. 2. [27]

$$F\,(\%) = \frac{F_i - F_0}{F_t - F_o} \times 100 \quad (2)$$

Where F_0, and F_i are fluorescence intensity at zero and t time respectively, and F is the percentage of fluorescence intensity. The fitting of the experimental data and independent variables were evaluated by using of a second order polynomial model obtained by Design Expert 7.0.0 software as follows:

$$Y = \beta_0 + \sum \beta_i X_i + \sum \beta_{ii} X_i + \sum \beta_{ij} X_i X_j + \in \quad (3)$$

Where response variable was predicted as *Y*, β_0 is the interception, the polynomial regression coefficients are as β_i, β_{ii} are quadratic coefficients, and β_{ij} are coefficients of the interaction. X_i and X_j imply the chosen independent variables and $\in$ is random errors.

3. Results and discussion

3.1. Characterization of the synthesized nano carrier

3.1.1. FT-IR spectra

In the magnetized polypyrrole core-shell (Fe_3O_4@PPY) spectrum (Fig. 1a), the absorption

band appeared at 470 cm^{-1} was attributed to the characteristic Fe-O band and the peak at 1400 cm^{-1} belonged to OH in-plane (O-H), and peaks appeared at 1600 and 3400 cm^{-1} related to water molecules absorbed on the surface of the sample. Besides the characteristic absorption bands of polypyrrole, the peaks appeared at 1000 and 1100 cm^{-1} were assigned to the CH in-plane, $(C\text{-}H)_{in}$ and CH out-of-plane, $(C\text{-}H)_{out}$ vibration [28]. The peaks around 1500 and 1474 cm^{-1} were respectively attributed to C-N and C-C asymmetric and symmetric ring-stretching of PPY [29]. The peak at 1400 cm^{-1} was attributed to the stretching band related to C=C of PPY ring. The weak absorption bands of NH and CH stretching vibration of polypyrrole appeared respectively at 3404 and 2358 cm^{-1} and the band at 3404 cm^{-1} was related to the symmetrical stretch vibration of NH group which was buried under board OH peak of water molecules at 3400 cm^{-1} [30]. In the FT-IR spectrum of the carrier (Fe_3O_4@PPY-MET-PEG) (Fig.1b), besides the absorption bands of Fe_3O_4@PPY, the bands related to MET and PEG were clearly observed.

The peaks belonged to MET were observed as following positions:

-The strong absorption band at 3160 cm^{-1} was attributed to C-H stretching of the ring. The absorption bands observed at 3127, 3108 and 2940 cm^{-1} were related to C-H stretching of methyl group, and the bans appeared at 1572 cm^{-1} was attributed to C-C stretching and ring C-H (N-H) bending. The absorption band at 1465 cm^{-1} was related to C-S stretching, ring CN stretching and ring NH bending [31]. The presence of PEG in the sample was indicated by the following absorption bands:

The C-O-C bond of ether was appeared at 1100-1060 cm^{-1}, and O-H stretching of hydroxyl group at 3400 cm^{-1}. The absorption band at 2900 cm^{-1} was attributed to C-H stretching of alkanes, the bands at 1450-1292 cm^{-1} were related to C-H scissor and bending. C-O stretching band of alcohol was appeared at 1250 cm^{-1} [32].

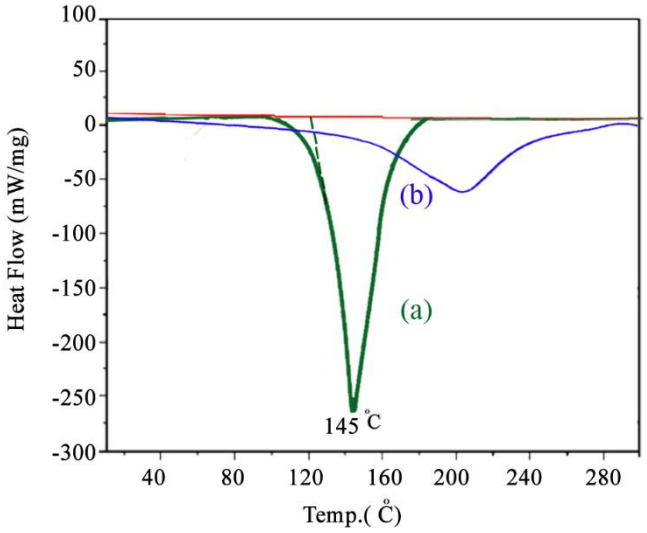

Fig. 1. FT-IR spectra of Fe_3O_4@PPY (a) and Fe_3O_4@PPY-PEG-MET (b)

3.1.2. DSC spectra

The DSC curves of MET given in Fig. 2a showed a sharp endothermic peak started from 80˚C and ending at 150˚C with a maximum at 145 ˚C which was attributed to the elimination of water molecules and melting of MET. In the DSC curve of Fe_3O_4@PPY-MET-PEG (Fig.2b), the endotherm belonged to the melting of MET was shifted to higher temperature owing to the complexation of MET with PEG and immobilization of the complex on the surface of Fe_3O_4@PPY. This peak started from 160 and ended at 290 ˚C with maximum at 250˚C. Such a shift has already been reported in similar works [33].

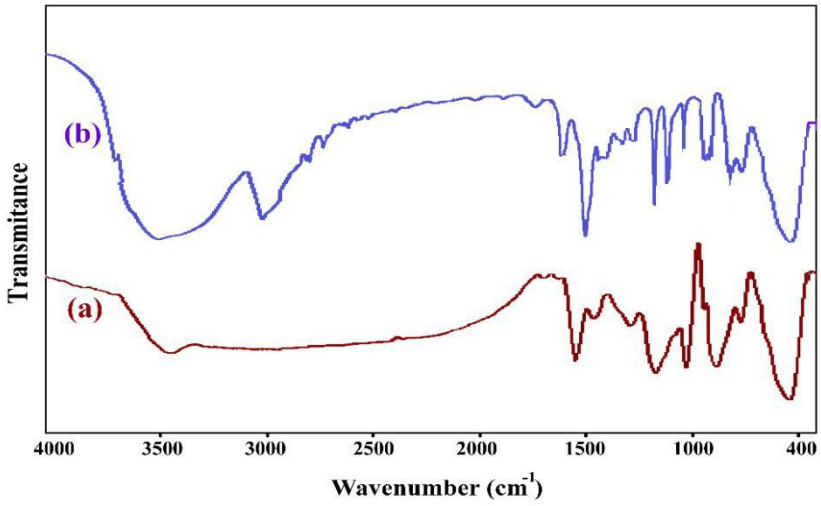

Fig. 2. The DSC curve of MET (a), and Fe3O4@PPY-PEG-MET (b)

3.2. Study of the variables influencing the release of MET

The nanocarrier prepared in this work was expected to improve the controlling and managing of the drug release through its various capabilities. PEG as a permeating agents improved the loading and release of the drug. By using carriers with different MET/PEG ratio, the effect can be optimized. The magnetization of the carrier which was performed in a simple and quick process, facilitated the easy separation of the carrier from the solution. Moreover, for in-vivo delivery tests the pathway of nano carrier can be scanned by magnetic resonance imaging (MRI) technique[34]. By this technique the magnetic nano carriers are easily detected and can be conducted to the target tissues of the body. The most drawbacks of nano-sized magnetic particles are the possible aggregation of the particles which decreases the effectiveness of the method, and also the low stability of the particles in high acidic and basic media. These limitation was eliminated by covering the magnetic core by biocompatible polymer; PPY that supported nanoparticles properties and also can be used in vivo drug release media. [35]

According to the quadratic equation of the CCD method, the most important influential parameters of the nanocarrier were the amount of MET and PEG considered as numerical factors respectively X1 and X2. The pH of the releasing media X3 was considered as categorical factor. The amount of Fe_3O_4 nanoparticle was constant in all studied samples.

The experimental range and levels of the independent variables are shown in Table 1. The amounts of MET and PEG as independent variables was respectively in the ranges of (0.01-0.04) and (0.00-0.04). These values were considered as numerical factors in term of alphas. The pH of media was considered as categorical factor in tow levels, 1.2 and 7.4.

Table 1. Experimental range and levels of independent process variables for nano carrier

Independent variables	Range and Levels				
	-α	-1	Mean	+α	+1
Drug (g)	0.010	0.0127	0.025	0.038	0.040

PEG (g)	-4.9E-08	0.003	0.020	0.037	0.040
pH	1.2			7.4	

As indicated in Table 2, the experiments for drug release in SGF and SBF medias was design in 26 run and two block. Two numerical factors, MET and PEG values entered in terms of alpha and 13 runs were obtained. Five center points and eight not center points was obtained. The center points removed random error of the experiments. Then by entering numerical factor, pH, in two levels 1.2 and 7.4, the number of runs become 26 run. The observed column in table 2 shows the amount of drug release which was obtained by the fluorescence intensity of the samples. The data in predicted column was given by the model according to the variables. The agreement between the observed data and predicted data indicated the significance of the model.

Table 2. Full factorial central composite design matrix for nano carrier production

Run	Block	Independent variables			Response (FL intensity)	
		Drug (g)	PEG (g)	pH	Observed	Predicted
1	Block 1	0.01	0	7.4	7.19E+05	7.29E+05
2	Block 1	0.02	0.02	1.2	3.71E+05	3.62E+05
3	Block 1	0.04	0.04	1.2	3.51E+05	3.56E+05
4	Block 1	0.01	0.04	7.4	7.55E+05	7.54E+05
5	Block 1	0.02	0.02	7.4	7.76E+05	7.73E+05
6	Block 1	0.04	0	1.2	3.62E+05	3.62E+05
7	Block 1	0.02	0.02	1.2	3.54E+05	3.62E+05
8	Block 1	0.01	0	1.2	3.37E+05	3.29E+05
9	Block 1	0.04	0	7.4	7.80E+05	7.78E+05
10	Block 1	0.01	0.04	1.2	3.37E+05	3.43E+05

11	Block 1	0.04	0.04	7.4	7.88E+05	7.83E+05
12	Block 1	0.02	0.02	7.4	7.72E+05	7.73E+05
13	Block 2	0.04	0.02	7.4	7.81E+05	7.87E+05
14	Block 2	0.01	0.02	1.2	3.38E+05	3.43E+05
15	Block 2	0.02	0.02	1.2	3.50E+05	3.67E+05
16	Block 2	0.02	0.02	7.4	7.76E+05	7.77E+05
17	Block 2	0.02	0	1.2	3.52E+05	3.61E+05
18	Block 2	0.02	0.02	7.4	7.70E+05	7.77E+05
19	Block 2	0.02	0	7.4	7.73E+05	7.66E+05
20	Block 2	0.04	0.02	1.2	3.69E+05	3.65E+05
21	Block 2	0.02	0.02	1.2	3.72E+05	3.67E+05
22	Block 2	0.02	0.02	1.2	3.78E+05	3.67E+05
23	Block 2	0.02	0.02	7.4	7.80E+05	7.77E+05
24	Block 2	0.01	0.02	7.4	7.58E+05	7.48E+05
25	Block 2	0.02	0.04	1.2	3.80E+05	3.69E+05
26	Block 2	0.02	0.04	7.4	7.78E+05	7.85E+05

The ANOVA results and full quadratic model are given in Table 3. The R^2 value of 0.9968 indicated that the data was successfully fitted into the model and the response variability was properly explained by the employed model. F-test and p-value were used as useful statistical tools to check the significance of each coefficients. The large F-value (1585.72) and small p-value (0.0001) determined by the model was considered as the more significant characters in the regression model [36,37].

The F-value of Lack of Fit is 0.68 implied that it was not significant relative to the pure error. Non-significant lack of fit indicated that the data was reasonably fitted to the model. The

signal to noise ratio greater than 4 was desirable and showed an adequate precision. The precision ratio of 51.67 obtained in this work was considered as an acceptable signal. The predicted R-Squared of 0.9888 was in reasonable agreement with the adjusted R-Squared of 0.9952 indicating that the experimental data were statistically fitted into the model were within 95% of confidence interval.

Table 3. ANOVA for Response Surface Quadratic Model

Source	Sum of Squares	df	Mean Square	F-Value	p-value Prob > F	
Block	6.04E+08	1	6.04E+08			
Model	1.11E+12	8	1.39E+11	1585.72	< 0.0001	significant
X1-Drug	1.87E+09	1	1.87E+09	21.42	0.0003	
X2-PEG	4.77E+08	1	4.77E+08	5.46	0.0327	
X3-pH	1.88E+11	1	1.88E+11	2154.11	< 0.0001	
X1X2	2.18E+08	1	2.18E+08	2.49	0.134	
X1X3	2.16E+08	1	2.16E+08	2.47	0.1358	
X2X3	9.29E+07	1	9.29E+07	1.06	0.3178	
X1^2	1.31E+09	1	1.31E+09	15.03	0.0013	
X2^2	1.74E+07	1	1.74E+07	0.2	0.6616	
Residual	1.40E+09	16	8.74E+07			
Lack of Fit	7.44E+08	10	7.44E+07	0.68	0.7171	not significant
Pure Error	6.54E+08	6	1.09E+08			
Cor Total	1.11E+12	25				

R^2 =0.9968, $R^2_{adjusted}$=0.9952, $R^2_{predicted}$=0.9888, Adequate precision=51.67

The fitted model for fluorescence response considered as the amount of released drug as a

function of the more significant variables is shown in Eqs. 4 and 5 at (pH=7.4) and (pH=1.2), respectively:

pH (7.4)*:* Y1 =6.82E+05 + 5.76E+06 MET + 9.93E+05 PEG - (4)
1.71E+07 MET*PEG -8.21E+07 MET^2 - 4.61E+06 PEG^2

pH (1.2)*:* Y2 =2.87E+05 + 5.21E+06 MET + 7.14E+05 PEG - (5)
1.71E+07 MET*PEG -8.21E+07 MET^2 - 4.61E+06 PEG^2

In order to investigate the interaction between different variables, the Pareto curves were constructed from the data obtained by experimental design[38] (Fig.3). The upward and downwards charts respectively showed the positive influence and negative effects on the model. According to the curves, the amount of MET (X1), amount of PEG (X2) and pH (X3) were the effective variables. The MET and PEG values had positive effect on the designed model. The quadratic interaction of drug (drug^2) and PEG (PEG^2) had negative effect on response values. When the amount of drug increased, the drug release was accelerated till the interaction of drug-drug caused aggregation of drug particles which lead to a significant decreased on the drug release. By study of interaction PEG^2, it was concluded that the release percentage of the drug was increased by gradual increasing of PEG amounts. However, further increase of PEG had negative effect on the drug release because of formation of a strong bond with the drug and the aggregation the molecules. But interactions X1X2 (Drug*PEG) had negative effect owing to the formation of MET-PEG complex which limited the release of the drug. These interactions was similar in SGF and SBF media indicating that the interactions are independent of the releasing media.

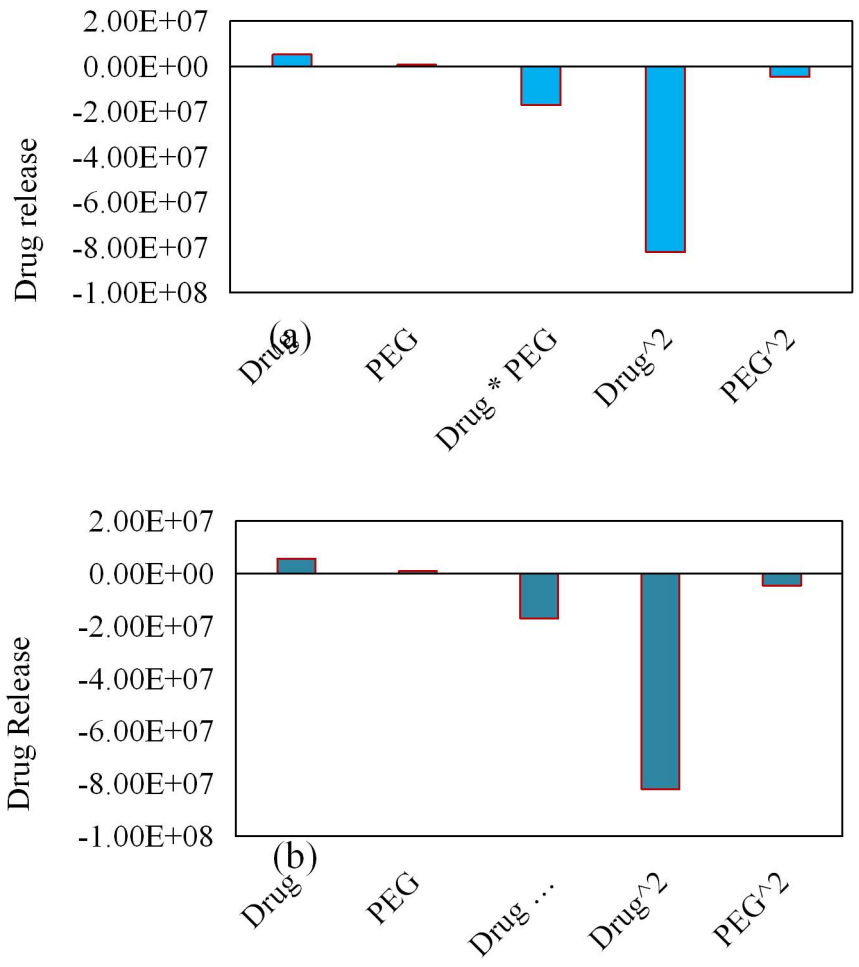

Fig. 3. Pareto curves in SGF (a) and in SBF (b)

3.3. Evaluation of influencing variables by 3D response surface plots

The graphical results of interactive effects of the variables are given as three dimensional (3D) response surface view in Figs. 4, and 5 respectively for SGF and SBF media. The plots represent the response for interactive variables; amounts of MET, and amount of PEG in the studied media. As indicated in the figure, with high amount of drug, owing to the aggregation of drug molecules, the release values was decreased and a negative effect was observed on the designed model. However, with gradual increasing of PEG amount the release value was increased.

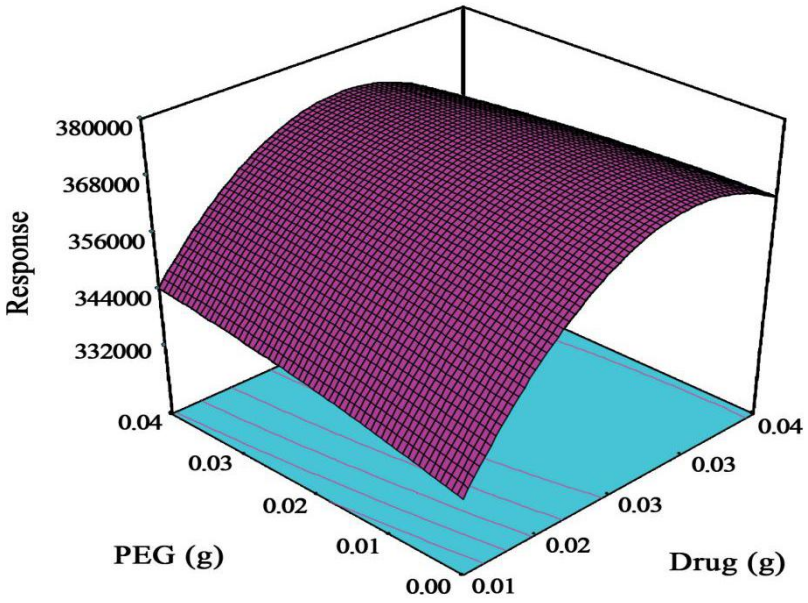

Fig. 4. 3D response surface curve at pH=1.2

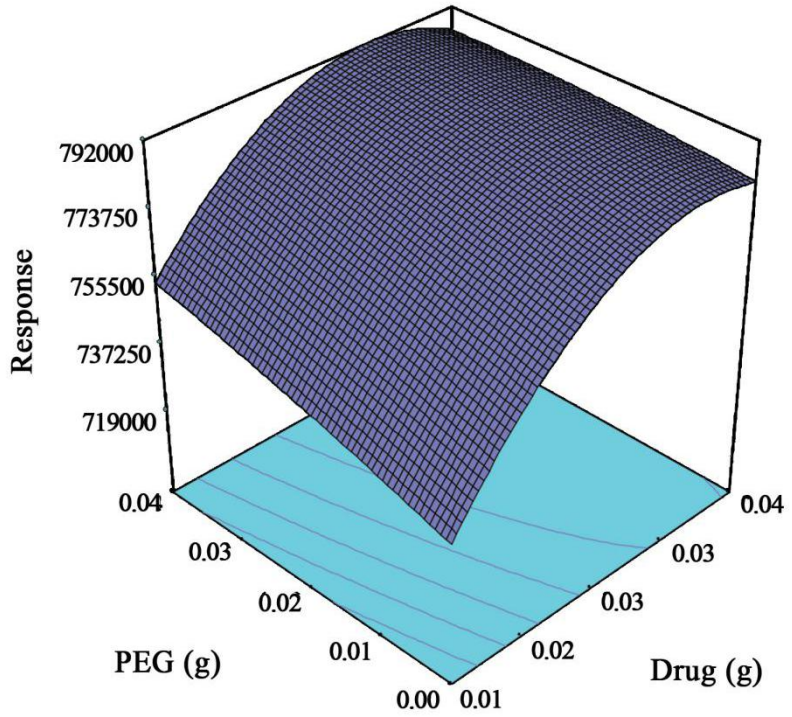

Fig. 5. 3D response surface curve at pH=7.4

The release values are more pronounced in SBF media compare to the values observed in SGF media. This was attributed to the protonation of thiol group of MET in acidic environment of SGF media creating a repulsive electrostatic force between positive MET and acidic media.

Charnay et al. studied in vitro release of ibuprofen into simulated gastric fluid and intestinal fluid. They reported that ibuprofen release into intestinal fluid (pH=7.4) was faster than in gastric fluid [39].

Manzano evaluated the release of ibuprofen from amine functionalized MCM-41, and un-functionalized silica particles. The amine-modified MCM-41 particles showed higher loading capacity and higher delivery [40].

3.4. Model Diagnostic Plots

The diagnostic tools for model confirmation investigate non-divergence of data proposed from each other and from the predicted model. The results of internally studentized residuals versus run did not show any tendency and the results show a random scatter within +3 to -3 ranges. The diagnostic tools checks to find if the variables may have influenced the response during the experiment. The trends indicated a time-related variable lurking in the background (Fig. 1Sa). The normal probability plot showed that the residuals had a normal distribution, and the points follow a straight line. Even the scatter data are within an acceptable tolerance (Fig.1Sb) [42].

The adequacy of the model was also examined from the plot of residuals versus the predicted values (Fig. 1Sc). The plot showed a random scatter with a constant variance.

The plot of the actual response versus the predicted response is represented in Fig. 1Sd. As indicated in the figure a value or a group of values, had sufficient tendency to the predicted values (Fig. 1Sd) [43].

Box Cox Plot for Power Transforms provides a guideline for selecting the correct power law transformation. Based on the best lambda (λ) value, which is found at the minimum point of the curve generated by the natural log of the sum of squares of the residuals. If the 95% confidence interval around this lambda includes 1 then the software does not recommend a specific transformation. This situation was accurately found in our experiments (Fig. 1Se).

The plot of the residuals versus block is given in Fig. 1Sf insignificant curvature of the plot indicated a random contribution of the independent factor that is accounted for by the model

(Fig. 1Sf).

3.5. Process optimization

Optimization of responses as a widely used approach in the RSM consists of switching the various responses into a single one through joining the response into a nanocarrier function and then its optimization[44]. In the suggested model, desirability in SGF media was close to 1 and in SBF media was equal to 1, confirming the fitness of the model. Optimum values of independent variables for maximum MET delivery were showed in the Table 4.

Table 4. Optimum values of factors

Independent variables			Maximum efficiency of drug release	
MET (g)	PEG (g)	pH	Drug release	Desirability
0.03	0.02	1.20	370093	0.92
0.02	0.02	7.40	783656	1.00

In this research, by use of RSM, the ingredients needed for the synthesis of nanocarrier was optimized and drug delivery in SGF and SBF media was investigated. The rate of drug delivery and selected sample for controlled and slow release was studied by the kinetic study of the process.

3.6. Kinetic study of the process

The fraction of cumulative release (X) at time "t" for in-vitro MET delivery obtained in 4 random run (samples, 8, 9, 16 and 20) are given in Fig. 6.

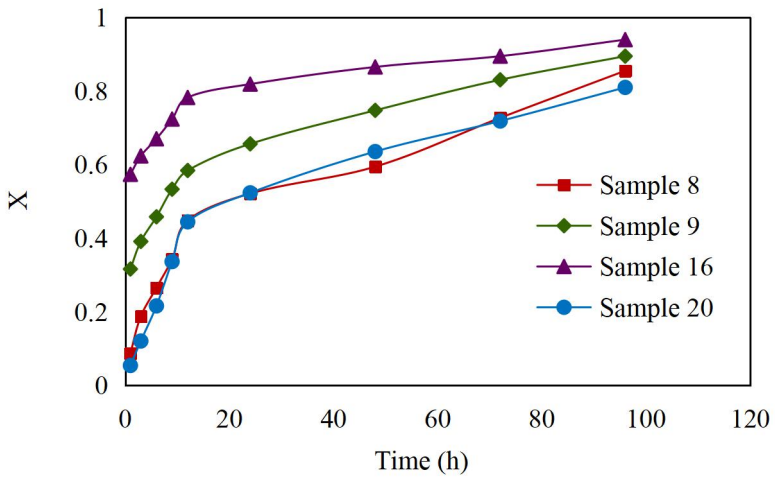

Fig. 6. Fraction of cumulative release of in-vitro MET delivery in samples 8, 9, 16 and 20

The kinetic of the delivery systems and its mechanism was studied by Ritger-Peppas and Avarim's models.

-Ritger-Peppas improved an experimental equation to determine both Fickian and non-Fickian drug release from swelling or non-swelling in-vitro delivery systems [44,45,46]. The equation is represented as:

$$X = kt^n \tag{6}$$

The logarithm form of equation is as follows:

$$Log(X) = Log(k) + nLog(t) \tag{7}$$

Where X is drug released fraction at "t" time, n is diffusion exponent that illustrate the mechanism of in-vitro drug release through the carrier, K is kinetic constant indicating the rate of the delivery system (Fig. 7). In Ritger-Peppas model, the release exponent, n=1 indicates the zero order release, where the release is independent of drug concentration. $n \leq 0.43$ indicates the Fickian diffusion release from non swellable matrix and if $0.43 < n < 1.0$ the release is non-Fickian in the nature, indicating that the drug release followed both diffusion and erosion controlled mechanisms[47].

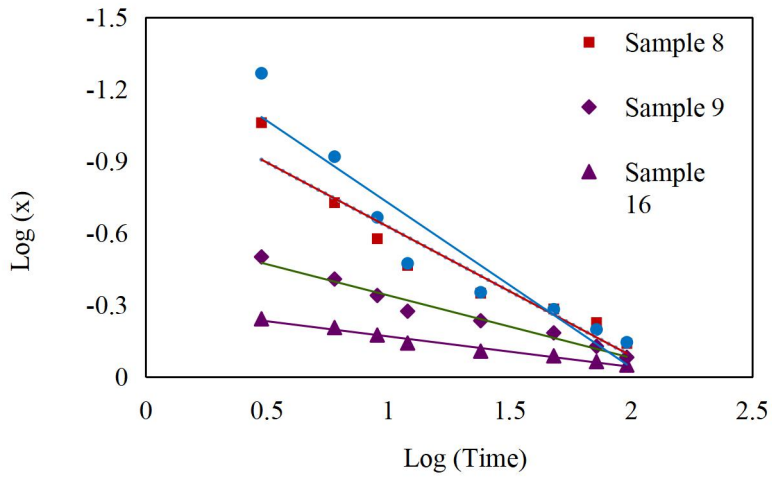

Fig. 7. The R-P curve for in-vitro MET delivery from Fe_3O_4@PPY-PEG-MET

Kinetic model parameters of Ritger-Peppas model of in-vitro MET delivery are given in Table 5. The results indicated that in samples 9 and 16, n was ≤ 0.43 in SBF media , indicating Fickian diffusion release and in samples 8 and 20 the n values was 0.43 < n < 1.0 for SGF media indicating non-Fickian release that followed the diffusion and erosion controlled mechanisms.

Table 5. Kinetic parameters of R-P and Avarim's models of MET Delivery

Sample	MET	PEG	pH	n_{R-P}	k_{R-P} (h^{-n})	n_{Avarim}	k_{Avarim} (h^{-n})	X
8	0.01	0.00	1.2	0.54	0.07	0.65	0.10	0.855454
9	0.04	0.00	7.4	0.26	0.25	0.42	0.32	0.895131
16	0.02	0.02	7.4	0.13	0.51	0.28	0.74	0.940121
20	0.04	0.02	1.2	0.69	0.04	0.74	0.06	0.810203

Peng and co-workers studied the release of naproxen from carbon nanotubes hydrogel. Their results was showed the release of drug into media with (pH=7.4) was faster than in (pH=1.2). This was confirmed by R-P kinetic model[48]. They indicated that Ritger-Peppas model conducted a Fick-diffusion process at (pH=1.2), while and at (pH=7.4) non-Fick diffusion process such as surface diffusion and corrosion diffusion processes was followed. They

suggested that this was related to the structure of naproxen, carrier and their interactions with realizing media [49]. The release process was also studied by Avarim's model[49,50].

A simple expression of Avarim's equation is given in Eq. 8:

$$X = 1 - exp\,(-kt^n) \quad (8)$$

Where X is the fraction of released at "t" time, k is the release rate constant and n is the Avarim's parameter for determination of release mechanism. Both k and n represent the value of release and are experimentally determined [51]. Eq. 8 can be rearranged by double logarithm to generate Eq. 9.

$$Ln(-Ln(1-X)) = Ln\,(k) - nLn\,(t) \quad (9)$$

By drawing a linear plot of ln (ln(1 -X)) vs. ln t (Eq. 9) k, the release rate constant and n as release parameter were obtained (Fig. 8).

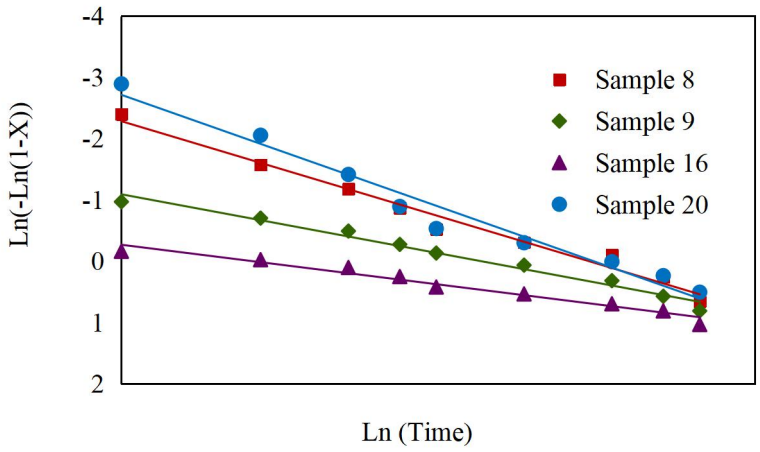

Fig. 8. The Avarim's curve for in-vitro MET delivery from Fe_3O_4@PPY-PEG-MET

n<1 representing diffusive release and n=1 corresponds to first-order kinetics[52]. The kinetic parameters Avarim's model are given in Table 5. In each samples n < 1 indicated the diffusive release of MET. The comparative kinetic constant, k, showed that the MET release in SGF media was significantly slower than in SBF media.

This fact was attributed to the influence effect of PEG that controlled MET delivery in SGF and caused the slow release in sample 20 rather to sample 8 that by increasing amount of PEG, the release value was decreased. MET delivery in SBF represented non-Fickian release and is

not controlled by PEG. Because by increasing of PEG and decreasing of MET in sample 16 rather than sample 9, release value was increased and illustrated that drug delivery was independent of PEG and PEG had not enhancing effect on controlled delivery.

4. Conclusion

In this research, the magnetic core-shell (Fe_3O_4@PPY) was sucessfully synthesized by in-situ oxidative polymerization and the synthesized core-shell was employed as a biocompatible nano carrier for in-vitro delivery of MET. The MET was loaded on the carrier as MET-PEG complex. The results indicated that the presence of of PEG had positive effect on the drug release and controlled rate in SGF media, but its effect in SBF media was insignificant.The effect of MET/PEG ratio on the releasing process was studied and it was concluded that the ratio of 2/1was the optimized value. The evalution of the interactions between variables indicated that MET and PEG interaction had positive effect on the designed model. The quadratic interaction of drug (drug^2) and PEG (PEG^2) had negative effect on the response values. The interactions Drug*PEG had also negative effect.

The releasing data were interpeted by applying R-P and Avarim kinetic models and it was concluded that in SGF, the release process was controlled by diffusion and erosion and rate of release (k) in this media was slower than SBF. This illustratted that PEG as enhancer, can control the MET release in SGF.

Conflicts of interest

There are no conflicts to declare.

Acknowledgements

This research was performed in the department of chemistry, Azad University, Shahreza Branch. The author wish to acknowledge its valuable co-operations.

References

[1] Flanders J. *Vet. Clin. North Am. Small Anim. Pract.* 1994, **24**, 607.

[2] Becker T, Graves K, Kruger M, Braselton E, Nachreiner F. *J. Am. Anim. Hosp. Assoc.* 2000, **36**, 215.

[3] Kalam A, Humayun M, Parvez N, Yadav S, Garg A, Amin S, Sultana Y, Ali A. *Release Continental J. Pharm. Sci.* 2007, **1**, 30.

[4] Ofoefule I., Chukwu A. Sustained release dosage forms: design and evaluation of oral products. In: Ofoefule S.I (ed.), Text Book of Pharmaceutical Technology and Industrial Pharmacy. Samakin (Nig.) Enterprises, Lagos 2002; 94-120.

[5] Shah U, Rehman A. *Pak. J. Pharm. Sci.* 2011, **24**, 183.

[6] Buijtels J, Kurvers I, Galac S, Winter E, Kooistra H. *16th ECVIM Annual Congress,* 2006, 14.

[7] Karawi A, Daraji A., *Polym.* 2010, **79**, 769.

[8] Liu C., Chen Y., Chen J., *Polym.* 2010, **79**, 500.

[9] Manchanda R., Fernandez-Fernandez A., Nagesetti A., McGoron A., *Colloids Surf. B.* 2010, **75**, 260.

[10] Fiore V., Lofton M., Roser-Page S., Yang S., Roman J., Murthy N., Barker T., *Biomaterials.* 2010; **31**: 810-817.

[11] Zheng X., Kan B., Gou M., Fu S., Zhang J., Men K., Chen L., Luo F., Zhao Y., Zhao X., Wei Y., Qian Z., *Int. J. Pharm*. 2010; **386** (2): 262-269.

[12] Regi M., Ramila A., Real R., Perez-Pariente *J., Chem. Mater*. 2001; **13**: 308–311.

[13] Doadrio A., Sousa E., Doadrio J., Perez-Pariente J., Barba I., Regi M., *J. Control. Rel.* 2004; **97**: 125-131.

[14] Regi M., Doadrio J., Doadrio A., Barba I., Perez-Pariente *J., Solid State Ionics* 2004; **172**: 435–439.

[15] Prajna M., Bismita N., Dey R, *Asian J. Pharma. Sci.* 2016; **11**: 337–348

[16] Francesco M. Veronese P., Gianfranco P., *Reviews Drug discovery today.* 2005; **10** (21):1451-1458.

[17] Riehemann K., Schneider S., Luger T., Godin B., Ferrari M., Fuchs H., *Angew. Chem. Int.*

Ed. 2009; **48**: 872- 897.

[18] Dinc C. Kibarer G., Guner A., *J. Appl. Polym. Sci.* 2010; **117**: 1100-1119.

[19] Chiou W. Riegelman S., *J. Pharm. Sci.* 1971; **60** (9):1281-1302.

[20] Serajuddin A., *J. Pharm. Sci.* 1999; **88** (10): 1058-1066.

[21] Leuner C., Dressman J., *Eur. J. Pharm. Biopharm.* 2000; **50**:47 – 60.

[22] Prakash B., Neelima A., Snehith V., Ramesh C., *Ars. Pharm.* 2009; **50** (1):8-23.

[23] Wang J., Zheng S., Shao Y., Liu J., Xu Z., Zhu D., *J. Colloid Interface Sci.* 2010; **349**:293–299.

[24] Ghosh A., Biswas S., Ghosh T., *J. Young Pharm.* 2011; **3**(3): 205–210.

[25] Ramesan M., *Int. J. Polym. Mater. Polym. Biomater.* 2015; **62**: 277–283.

[26] Rockville M., *J. pharma. Sci.* 1993; **82**: 1580-1594.

[27] Shamaeli E., Alizadeh N., *Electrochimica. Acta.* 2013; **114**:409-415

[28] Turcu R., Pana O., Nan A., Craciunescu I., Chauvet O., Payen C., *J. Phys. D: Appl. Phys.* 2008; **41**: 1–9.

[29] Lamprakopoulos S., Yfantis D., Yfantis A., Schmeisser D., Anastassopoulou J., Ophanides T., *Synth. Met.* 2004; **14**: 229–234.

[30] Zhao S., Lee D., Kim C., Cha H., Kim Y., Kang Y., *Bull. Korean Chem. Soc.* 2006; **27**: 237-242.

[31] Biswas N., Thomas S., Sarkar A., Mukherjee T., Kapoor S., *J. Phys. Chem. C.* 2009; **113**: 7091-7100.

[32] Khairuddin E., Pramono S., Utomo V., Wulandari A., Zahrotul F., *J. Phys.: Conf. Ser.* 2016; **776**: 12053-12061.

[33] Kuru A., Aksoy S., *Textile Res. J.* 2014; **84**: 337-339

[34] Babincova M., Babinec P., *Biomed Pap Med Fac Univ Palacky Olomouc Czech Repub.* 2009; **153**(4):243–250.

[35] Uhrich K., Cannizzaro S., Langer R., Shakesheff K., *Chem. Rev.* 1999; **99**: 3181-3198.

[36] Doran B., Yetilmezsoy K., Murtazaoglu S., *Eng. Struct.* 2015; **88**: 74-91.

[37] Yetilmezsoy K., Demirel S., Vanderbei R.J., *J. Hazard. Mater.* 2009; **171**: 551-562.

[38] Pareto S., Gendy E, Hekmat R., Madian S, Salem S. Abu A., *Int. J. Microbiol.* 2013,

2013, 9.

[39] Charnay C., Begu S., Tourne-Peteilh C., Nicole L., Lerner A., Devoiselle J., *Eur. J. Pharm. Biopharm.* 2004, **57**, 533.

[40] Manzano M., Aina V., Arean C.O., Balas F., Cauda V., Collila M., Delgado M., Regi M., *Chem. Eng. J.* 2008, **137**, 30.

[41] Behbahani M, Moghaddam M, Arami M., *Desalination.* 2011, **271**, 209.

[42] Sadri Moghaddam S, Alavi Moghaddam M, Arami M, *J. Environ. Manag.* 2011, **92**, 1284.

[43] Fitrianto A., Midi H., *J. Sci. Technol.* 2012, **4**, 1.

[44] Korsmeyer R., Peppas N., *J. Control Rel.* 1983, **1**, 89.

[45] Ritger P. Peppas N., *J. Cont. Rel.* 1987, **5,** 23.

[46] Ritger P. Peppas N., *J. Cont. Rel.* 1987, **5**, 37,

[47] Singh J., Gupta S. Kaur H. *Sci. Res.* 2011, **6**, 400,

[48] Xiahui P., Qiang Z., Dongming P., Qiuli D. , Lini T., Feipeng J., Linqi L., jingyu L. , Chenxi Z. and Xiaomei W., *Iran. J. Pharm. Res.* 2013, **12**, 581,

[49] Avrami M., *J. Chem. Phys.* 1940, **8**, 212.

[50] Lorenzo A., Arnal M., Albuerne J., Muller A., *Polym. Test.* 2007, **26**:222.

[51] Kytariolos J., Dokoumetzidis A., Macheras P., *Eur. J. Pharm. Sci.* 2010, **41**,299.

[52] Shiga H., Yoshii H., Nishiyama T., Furuta T., Forssele P., Poutanen K., *Dry. Technol.* 2001; **19**: 1385.